Electronic Supplementary Information (ESI) available:

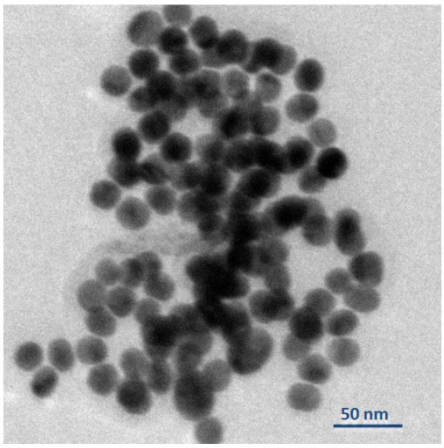

Figure S1 TEM image of $NaYF_4$ UCNPs.

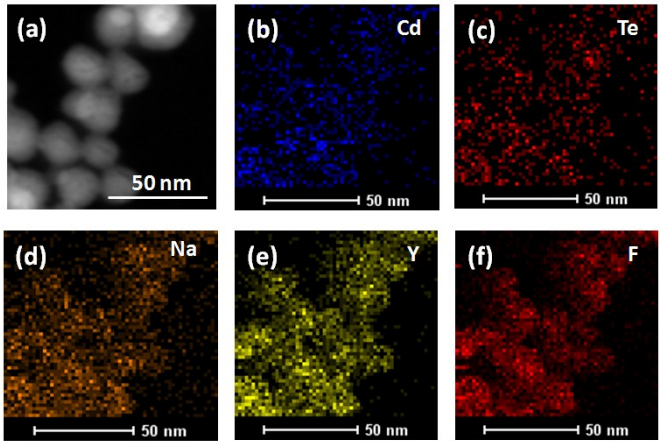

Figure S2 (a) TEM and (b-f) Elemental mappings of $NaYF_4$/CdTe QDs.

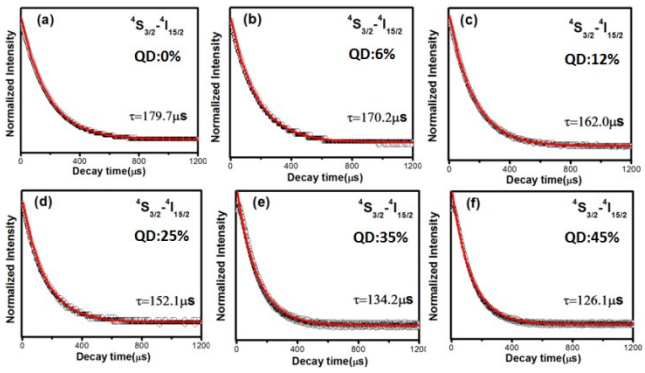

Figure S3 Dynamic curves of $^4S_{3/2}$-$^4I_{15/2}$ transition of Er^{3+} at different QD1 concentration under 980 nm light excitation.

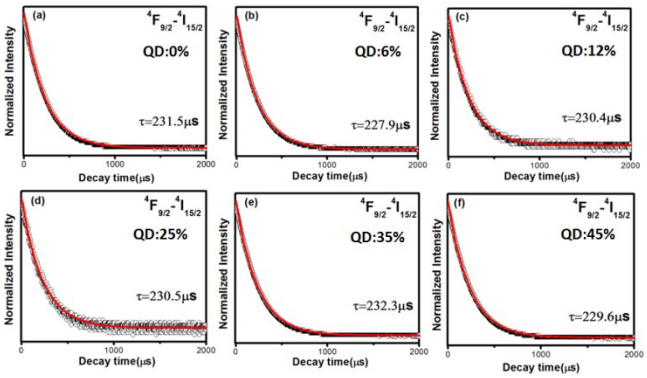

Figure S4 Dynamic curves of $^4F_{9/2}$-$^4I_{15/2}$ transition of Er^{3+} at different QD1 concentration under 980 nm light excitation.

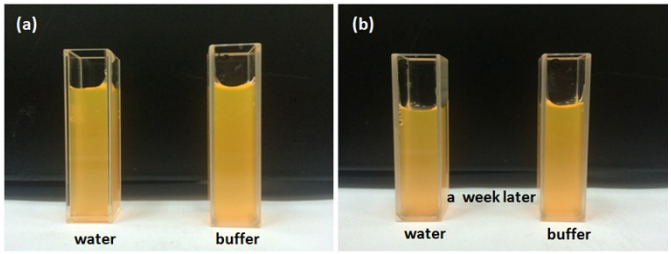

Figure S5 (a) The photograph of the complex of UCNPs and QDs (The concentration of the QDs is 45%) in water or buffer solution; (b) The photograph of the complex of UCNPs and QDs (The concentration of the QDs is 45%) in water or buffer solution after a week.

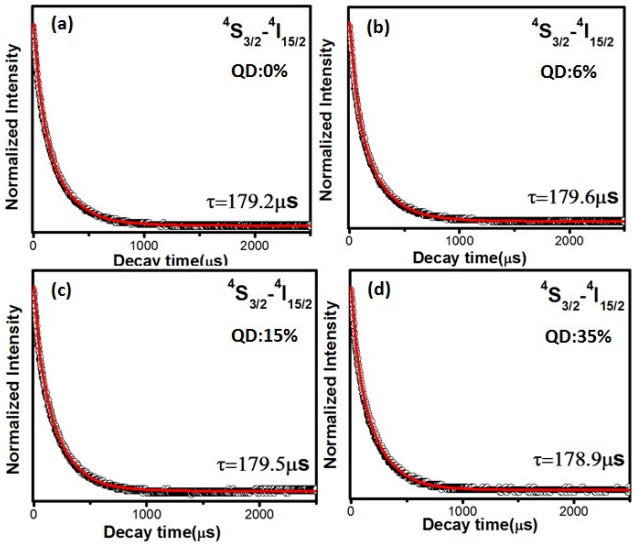

Figure S6 Dynamic curves of $^4S_{3/2}$-$^4I_{15/2}$ transition of Er^{3+} at different QD2 concentration under 980 nm light excitation.

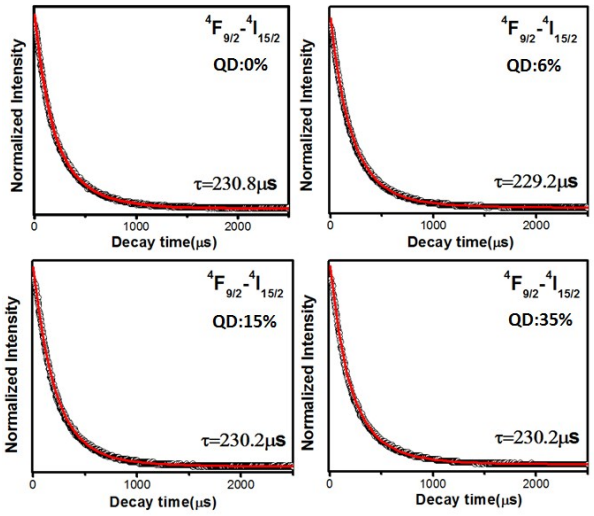

Figure S7 Dynamic curves of $^4F_{9/2}$-$^4I_{15/2}$ transition of Er^{3+} at different QD2 concentration under 980 nm light excitation.

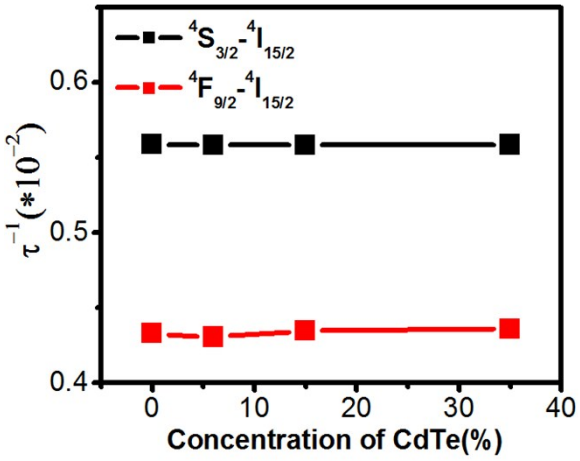

Figure S8 Inverse of the $^4S_{3/2}$, $^4F_{9/2}$-$^4I_{15/2}$ transition decay time at different QD2 concentration under 980 nm light excitation.

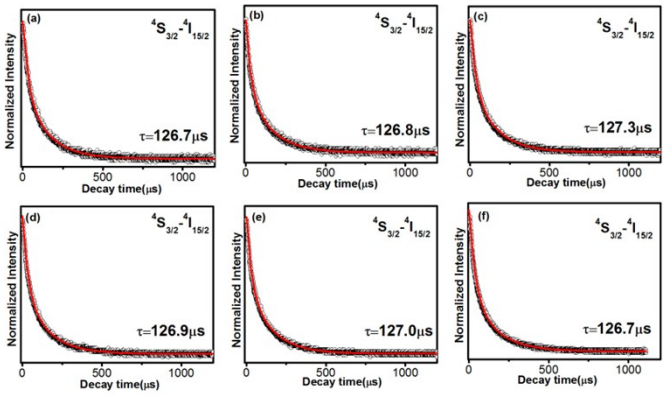

Figure S9 Dynamic curves of $^4S_{3/2}$-$^4I_{15/2}$ transition of Er^{3+} at different Hg^{2+} concentration under 980 nm light excitation in the human serum.

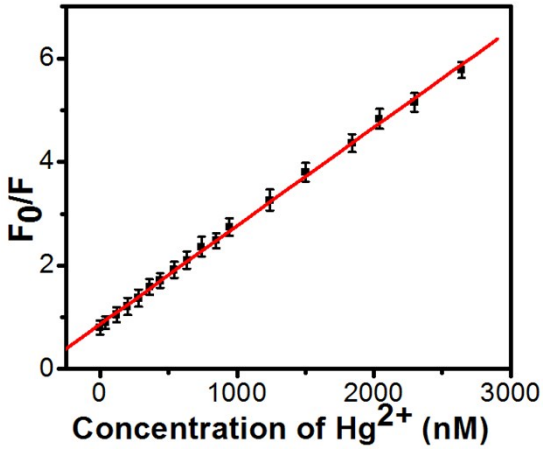

Figure S10 Fluorescence intensity ratio of FRET sensor as a function of Hg^{2+} concentration detected in human serum (0.15 g/mL).

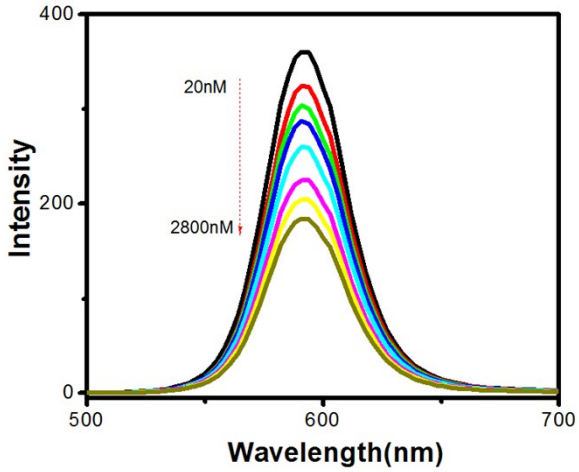

Figure S11 Fluorescence spectra of QDs with addition of various Hg^{2+} concentrations in PBS buffer.